

Operation of the jet feedback mechanism (JFM) in intermediate luminosity optical transients (ILOTs)

Amit Kashi¹ and Noam Soker²

¹ Minnesota Institute for Astrophysics, University of Minnesota, 116 Church St. SE. Minneapolis, MN 55455, USA; kashi@astro.umn.edu

² Department of Physics, Technion – Israel Institute of Technology, Haifa 32000, Israel; soker@physics.technion.ac.il

Received 2015 December 15; accepted 2016 February 22

Abstract We follow the premise that most intermediate luminosity optical transients (ILOTs) are powered by rapid mass accretion onto a main sequence star, and study the effects of jets launched by an accretion disk. The disk is formed due to large specific angular momentum of the accreted mass. The two opposite jets might expel some of the mass from the reservoir of gas that feeds the disk, and therefore reduce and shorten the mass accretion process. We argue that by this process ILOTs limit their luminosity and might even shut themselves off in this negative jet feedback mechanism (JFM). The group of ILOTs is a new member of a large family of astrophysical objects whose activity is regulated by the operation of the JFM.

Key words: stars: intermediate luminosity optical transients

1 INTRODUCTION

The heterogeneous group (Kasliwal 2011) of eruptive stars with peak luminosity below those of supernovae (SNe) and above those of novae (e.g. Mould et al. 1990; Rau et al. 2007; Ofek et al. 2008; Prieto et al. 2009; Botticella et al. 2009; Smith et al. 2009; Berger et al. 2009b; Kulkarni & Kasliwal 2009; Mason et al. 2010; Pastorello et al. 2010; Kasliwal et al. 2011; Tylenda et al. 2013; Kasliwal 2013) has been growing in recent years (Kasliwal 2013). Excluding low luminosity SNe and similar objects, such as Ca-rich transients and Type Ia SNe, the rest of the eruptive events are part of a group of so called intermediate luminosity optical transients (ILOTs; Berger et al. 2009b).

ILOT events of systems that harbor asymptotic giant branch (AGB) or extreme-AGB (ExAGB) pre-outburst stars, like NGC 300 OT2008-1 (NGC 300 OT; Monard 2008; Bond et al. 2009; Berger et al. 2009b) and SN 2008S (Arbour & Boles 2008), were studied both in the frame of single star models (e.g., Thompson et al. 2009; Kochanek 2011) and binary stellar models (Kashi et al. 2010; Kashi & Soker 2010b; Soker & Kashi 2011, 2012, 2013). Recent observations cast doubt that the progenitor star survived these events (Adams et al. 2015). McIcley & Soker (2014) conclude that single-star models for ILOTs of evolved giant stars encounter severe difficulties, and that ILOTs are most likely powered by a binary interaction. Here, we continue with developing and exploring the binary model for *all* ILOTs as we outlined in an earlier paper (Kashi & Soker 2010b).

In Kashi & Soker (2010b) we developed the High-Accretion-Powered ILOT (hereafter, HAPI) model. The HAPI model suggests that many (most) ILOTs are powered by a high-accretion rate event onto a main sequence (MS) star or a star that is slightly evolved off the MS, in a binary system. In some cases the binary system is actually a triple star system, where the tertiary star induces orbital instabilities and causes the two inner stars to interact. In this mass transfer event the accreted mass possesses high specific angular momentum to form an accretion disk, or an accretion belt, around the MS star (Kashi & Soker 2009). The accretion disk can launch two opposite jets that expel more mass from the system to form an expanding bipolar nebula (Kashi & Soker 2010a), such as the bipolar nebula associated with η Car, the Homunculus Nebula, that was formed in the Great Eruption (GE; e.g., Humphreys & Martin 2012 and references therein). The connection between some ILOTs and bipolar planetary nebulae (PNe) was mentioned in the past (Soker & Kashi 2012; Akashi & Soker 2013) in regards to the binary model for ExAGB-ILOTs. Prieto et al. (2009) already found a connection between NGC 300 OT and pre-PNe. The connection between some bipolar PNe and some ILOTs has gained support in recent years (e.g., Boumis & Meaburn 2013; Clyne et al. 2014; De Marco et al. 2014; De Marco 2015a,b; Zijlstra 2015).

In this paper we update the classification and grouping of ILOTs (Sect. 2) to further emphasize the common properties they share, including the presence of jets. In Section 3 we turn to propose that in some ILOTs the jets

lead to a negative jet feedback mechanism (JFM). We compare some properties of the JFM in ILOTs to those in other systems where the JFM operates. Our short summary is in Section 4.

2 ILOTS

2.1 The Energy-Time Diagram

The objects studied here (gap objects that are not SNe) can be classified in the following way.

ILRT: Intermediate-Luminous Red Transients. These are events resulting from evolved stars, such as AGB and ExAGB stars, and similar objects, e.g., red giant branch (RGB) stars. Most likely a companion accretes mass and the gravitational energy powers the eruption, e.g., NGC 300 OT. A similar process occurs in giant eruptions of luminous blue variables (LBVs).

LBV giant eruptions and SN Impostors. Giant eruptions of LBVs. Examples include the 1837–1856 GE of η Car and the pre-explosion eruptions of SN 2009ip. ILRTs are the low mass relatives of LBV giant eruptions.

LRN or RT: Luminous Red Novae, Red Transients or Merger-bursts. These are powered by a full merger of two stars. The process of destruction of the less dense star onto the denser star releases gravitational energy that powers the transient. Examples include V838 Mon and V1309 Sco. Merger events of stars with sub-stellar objects are also included.

ILOT: Intermediate-Luminosity Optical Transients. ILOT is the term for the combined three groups listed above (ILRT, LRN and LBV giant eruptions). These events, we argue, share many common physical processes, in particular being powered by gravitational energy released in a high-accretion rate event, the HAPI model.

We emphasize again that the definition of ILOT does not include low luminosity SNe or similar objects, such as Ca-rich transients and Type Ia SNe (for these see Kasliwal 2013).

A panoramic way to examine and compare ILOTs and other transient events is by using the Energy Time Diagram (ETD), as presented in Figure 1. (For a diagram showing peak luminosity rather than total energy versus the duration of the event, see, e.g., Kulkarni et al. 2007 and Kasliwal 2013.) The diagram shows the total energy of the transient as a function of its duration. Both the energy and the duration are not easy to define. The total energy includes both the integrated luminosity (radiated energy) and the kinetic energy that went to the ejected material. The radiated energy is calculated by integration of the lightcurve in the optical bands. The bolometric radiated energy is then calculated using a bolometric correction that is not always accurate. The kinetic energy is not easy to derive from observations and may be a few times larger than the radiated energy. It results in a range of possible energies, which is presented by an error bar in the ETD.

In some cases the energy that is missed by observations, i.e., the total available energy minus that emit-

ted in the optical band, can be large. This is the case for V838 Mon, where the energy required to inflate the envelope, marked by the black asterisk in Figure 1, is more than 10 times larger than that carried by radiation (Tylenda & Soker 2006). To account for the total *available* energy we calculate and present the gravitational energy released by the accreted mass, as described in eq. (5) of Kashi & Soker (2010b). This energy is marked by a black asterisk in the ETD. The advantage of doing so is that the total available energy better reflects the physical processes behind the transient, as according to our model these transient events are powered by gravitational energy. However, the total energy is estimated using a detailed model, and those models were derived for only a fraction of all transient events.

The ILOT timescale is defined typically as the time from its peak luminosity until it reaches its pre-ILOT luminosity, before the rise. (Using a criterion like a decrease by 3 magnitudes will not change the graph much.) Ideally it is defined for the bolometric luminosity, and as observations are limited, the waveband that contains most of the energy is used.

The ILOTs are found to lie on a wide stripe in the ETD – the Optical Transients Stripe (OTS). The stripe is not just an accidental position, and it has roots in accretion physics, as we demonstrate in Section 2.2 below. Transient objects positioned on the OTS have shared characteristics of being ILOTs, and in most cases their properties suggest that the transient is powered by gravitational energy, and belongs to the ILOT group.

In previous papers we reported different ILOTs that lay on the OTS (Kashi & Soker 2010b; Bear et al. 2011; Soker & Kashi 2011, 2012). The ETD presented in Figure 1 is updated with a number of recent ILOTs, as listed below.

- (1) **SN 2009ip.** An LBV that suffered several eruptions before (e.g., Berger et al. 2009a; Maza et al. 2009; Drake et al. 2012; Levesque et al. 2014; Mauerhan et al. 2013; Pastorello et al. 2013) its last one in 2012 (Margutti et al. 2014; Martin et al. 2015), that might have been a real SN explosion (Smith et al. 2014). There is also a possibility that the last 2012 eruption was an exceptionally strong giant eruption as well (Soker & Kashi 2013; Kashi et al. 2013). The calculated location of the sub-eruptions in 2011 and the two in 2012 (2012a and 2012b), as well as the total three years of activity (SN 2009ip Tot), are marked in Figure 1. It has been assumed that the total energy is twice the radiated energy for all eruptions of SN 2009ip.
- (2) **SN 2010mc.** This SN had a pre-explosion outburst about a month before explosion (Ofek et al. 2013). Soker (2013b) proposed that the pre-explosion outburst was powered by accretion onto an MS companion.
- (3) **R71 (HDE 269006).** A giant eruption of an LBV. Energy is calculated based on Mehner et al. (2013).

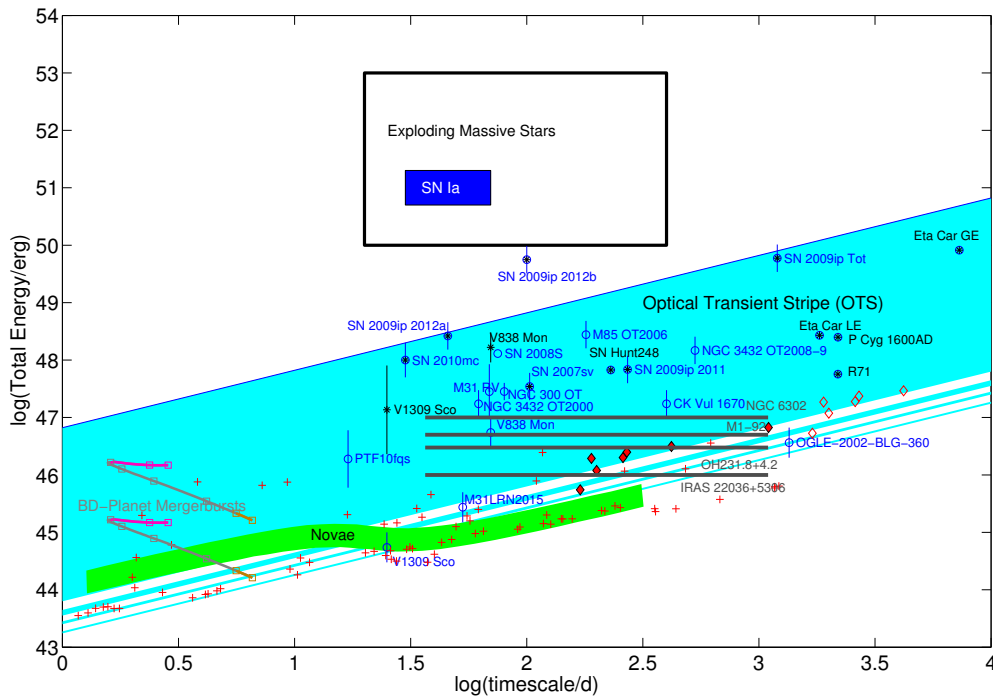


Fig. 1 Observed transient events on the ETD. Blue empty circles represent the total (radiated plus kinetic) energy of the observed transients as a function of the duration t of their eruptions. The OTS is an approximately constant luminosity region in the ETD. It is populated by ILOTs of different kinds: ILRTs, LRNs and LBV giant eruptions, i.e. SN impostors. It also includes predicted BD-planets merger-bursts (Bear et al. 2011). The upper limit of the OTS is constrained by Eq. (4). The green line represents nova models computed using the luminosity and duration from della Valle & Livio (1995). Nova models from Yaron et al. (2005) are marked with red crosses, and models from Shara et al. (2010) are represented with diamonds. The total energy does not include the energy which is deposited in lifting the envelope that does not escape from the star. For ILOTs that have a model to estimate the gravitational energy released by the accreted mass (the available energy), they are marked by black asterisks. PNe that might have been created in ILOT events are marked with gray horizontal lines, indicating the uncertainty in their ILOT event durations (Soker & Kashi 2012).

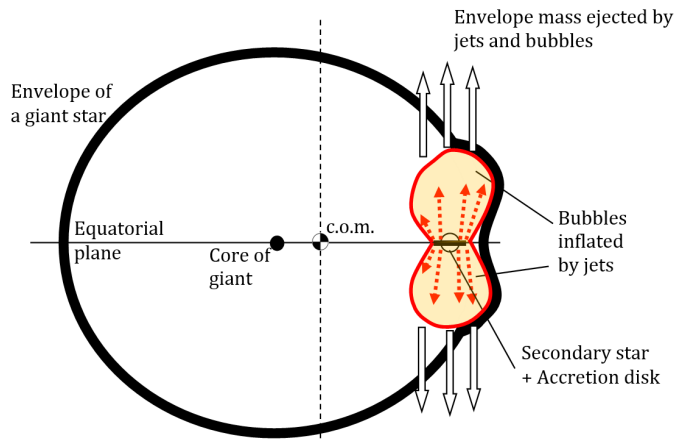


Fig. 2 A schematic flow structure of GEE. The companion accretes mass through an accretion disk and launches two jets in the outskirts of the giant envelope. The jets inflate bubbles and efficiently remove most of the envelope mass residing above and below the secondary orbit. A large fraction of this mass is located not far from the axis through the center of mass, depicted by a dashed line perpendicular to the orbital plane, and hence possesses a low value of specific angular momentum.

Late time data are missing so the location may be somewhat more to the upper right (longer duration and more energy), but certainly within the OTS.

(4) **CK Vul (Nova Vul 1670)**. A historic eruption showing three peaks between 1670 and 1672 (Shara et al. 1985). Hajduk et al. (2013) and Kamiński et al. (2015) suggested it might have been an ILOT. We used his-

toric data to position it on the ETD. Observations of a bipolar nebula (Hajduk et al. 2007) suggest the activity of jets.

- (5) **OGLE-2002-BLG-360**. Tylanda et al. (2013) claim it to be an ILOT (an LRN).
- (6) **SN2007sv**. This seems to be an SN impostor according to the analysis of Tartaglia et al. (2015). We find it to be at the center of the OTS. The total radiated energy is more than an order of magnitude below that of typical SNe. Since more than 7 years have passed since the outburst (ILOT event) and no SN explosion took place, this ILOT is not excited by oxygen burning in the core of a massive star. Its location on the OTS shows that it is an SN impostor with short duration and low energy.
- (7) **M31LRN 2015**. A recent LRN (Williams et al. 2015).
- (8) **SN Hunt248**. This SN impostor experienced an eruption with three peaks and returned to its pre-eruption luminosity in about 230 days (Kankare et al. 2015 and references therein). Its position in the ETD is close to that of the first 2012 peak of SN 20009ip.

2.2 The High-Accretion-Powered ILOT (HAPI)

Model

The most significant property ILOTs share according to the HAPI model is that the energy source is gravitational. A high accretion rate \dot{M}_a onto an MS or a slightly evolved off-MS star accounts for the high luminosity. Here we explore some of the implications of the HAPI model.

Let M_a and R_a be the mass and radius of the star accreting the mass, respectively. Star ‘*b*’ is the one that supplies the mass to the accretion; it is possibly an MS star that is completely destroyed, as in V838 Mon and V1309 Sco, or alternatively an evolved star in an unstable phase of evolution that loses a huge amount of mass, as in the GE of η Car. The average total gravitational power is the average accretion rate multiplied by the potential well of the accreting star

$$L_G = \frac{GM_a \dot{M}_a}{R_a}. \quad (1)$$

The accreted mass will plausibly form an accretion disk or an accretion belt. The accretion time ought to be longer than the viscous timescale for the accreted mass to lose its angular momentum. The viscous timescale is

$$t_{\text{visc}} \simeq \frac{R_a^2}{\nu} \simeq 73 \left(\frac{\alpha}{0.1}\right)^{-1} \left(\frac{H/R_a}{0.1}\right)^{-1} \left(\frac{C_s/v_\phi}{0.1}\right)^{-1} \times \left(\frac{R_a}{5 R_\odot}\right)^{3/2} \left(\frac{M_a}{8 M_\odot}\right)^{-1/2} \text{ days}, \quad (2)$$

where $\nu = \alpha C_s H$ is the viscosity of the disk, H is the thickness of the disk, C_s is the sound speed, α is the disk viscosity parameter, and v_ϕ is the Keplerian velocity. We scale M_a and R_a in Equation (2) to conform with the parameters of V838 Mon (Tylanda et al. 2005). For these parameters, the ratio of viscous to Keplerian timescale is $\chi \equiv t_{\text{visc}}/t_K \simeq 160$.

The accreted mass is determined by the details of the binary interaction process, and varies for different objects. We scale it by $M_{\text{acc}} = \eta_a M_a$. Based on the modeled systems (V838 Mon, V 1309 Sco, η Car) this mass fraction is $\eta_a \lesssim 0.1$ with a large variation. The value of $\eta_a \lesssim 0.1$ can be understood as follows. If the MS star collides with a star and tidally disrupts it, as in the model for V838 Mon (Tylanda & Soker 2006; Soker & Tylanda 2006), the destroyed star is likely to be less massive than the accretor $M_{\text{acc}} \lesssim M_b \lesssim 0.3 M_a$. In another possible case an evolved star loses a huge amount of mass, but the accretor only gains a small fraction of the ejected mass, as in the GE of η Car.

The viscous timescale gives an upper limit on the accretion rate

$$\dot{M}_a < \frac{\eta_a M_a}{t_{\text{visc}}} \simeq 4 \left(\frac{\eta_a}{0.1}\right) \left(\frac{\alpha}{0.1}\right) \left(\frac{H/R_a}{0.1}\right) \left(\frac{C_s/v_\phi}{0.1}\right) \times \left(\frac{R_a}{5 R_\odot}\right)^{-3/2} \left(\frac{M_a}{8 M_\odot}\right)^{3/2} M_\odot \text{ yr}^{-1}. \quad (3)$$

The maximum gravitational power is therefore

$$L_G < L_{\text{max}} = \frac{GM_a \dot{M}_a}{R_a} \simeq 7.7 \times 10^{41} \left(\frac{\eta_a}{0.1}\right) \left(\frac{\chi}{160}\right)^{-1} \times \left(\frac{R_a}{5 R_\odot}\right)^{-5/2} \left(\frac{M_a}{8 M_\odot}\right)^{5/2} \text{ erg s}^{-1}, \quad (4)$$

where we replaced the parameters of the viscous timescale with the ratio of viscous to Keplerian time χ . Equation (4) determines the upper bound on the OTS in the ETD. The upper bound might be crossed if the accretion efficiency η is higher and/or the stellar parameters of the accreting star are different. For most of the ILOTs the accretion efficiency is lower, hence they are located below this line, giving rise to the relatively large width of the OTS. The uncertainty in η_a is large and may be even above unity, but only in extreme cases. Therefore, we seldom expect to find objects slightly above the upper limit.

2.3 Implications of Accretion Powered Events

Adopting the premise that ILOTs are powered by a high mass accretion rate, the HAPI model, a great deal can be learned about them. We provide three examples.

The stellar masses of the two stars composing the η Car system were constrained using that model. The GE of η Car was initiated by close interaction with the eccentric companion close to periastron passages (Kashi & Soker 2010a). Daminieli (1996) tried to support the existence of a periodical variation using historical data, but claimed it cannot be done due to poor confidence in the data. Our calculation worked in an opposite way – we used the available historical lightcurve to develop a model and calculate the stellar and orbital parameters.

According to the model of Kashi & Soker (2010a), tidal forces of the companion disrupt the LBV that was in an unstable state, having an Eddington factor close to 1. According to the HAPI model, the luminosity peaks of the GE resulted from accretion onto the companion close to periastron passages (Kashi & Soker 2010a). Those peaks are ~ 5.1 years apart, while the present orbital period is ~ 5.54 years, suggesting that during the GE in the 1840s, the orbital period was shorter. Changes in orbital period most likely came from mass loss by the erupting system (enlarging the period), and accretion from the more massive LBV to the companion (shortening the period). Kashi & Soker (2010a) found that the only way for the HAPI mechanism to work within changes imposed by the orbital constraints requires the two stars to have significantly larger masses than initially thought. Instead of a binary system composed of an LBV with a mass of $M_1 \approx 120 M_\odot$ and a companion of $M_2 \approx 30 M_\odot$, the masses should be in the range $M_1 \approx 170 - 200 M_\odot$ and $M_2 \approx 80 M_\odot$. Based on the results of Figer et al. (1998) a zero-age main sequence (ZAMS) star with an initial mass of $M_{\text{ZAMS}} \approx 230 M_\odot$ is required to explain the present luminosity of the primary of η Car. The massive primary star deduced here is expected to result from a somewhat more massive ZAMS star, compatible with $M_{\text{ZAMS}} \approx 230 M_\odot$. However, this cannot be said for a present primary mass of $120 M_\odot$.

The accretion of the mass ejected from the primary onto the secondary formed a disk and launched jets. These jets had two effects: (1) They shaped the Homunculus Nebula into a bipolar nebula; and (2) they may have cleared some of the mass in the vicinity of the companion, thereby reducing the amount of available gas for further accretion, through the JFM discussed in Section 3.

A similar idea was applied to the LBV star P Cyg. There is no observed companion to P Cyg. Adopting the HAPI model and analyzing the peaks in its historical lightcurve, Kashi (2010) concluded that a 3–6 M_\odot binary companion in an eccentric orbit most likely does exist. The periastron passages of the companion caused the LBV to lose mass, part of which was accreted by the companion, releasing energy. The whole process modified the orbital parameters, resulting in a present period of ~ 7 years. The nebula around P Cyg has bi-axial features that may have been a result of relatively weak jets launched from the proposed companion during the outbursts. If such a companion is not found, it is possible that it was swallowed by the LBV star.

Soker & Kashi (2012) proposed that a number of bipolar PNe may have undergone ILOT events. Some PNe, such as NGC 6302 and the pre-PNe OH231.8+4.2, M1-92 and IRAS 22036+5306 have bipolar features that were formed in a rapid mass ejection event (e.g., Meaburn et al. 2008; Szyszka et al. 2011). The formation of a bipolar nebula in an event lasting weeks to years is a prediction of the HAPI model. The interaction with an MS companion causes the AGB (or extreme AGB) to lose a huge amount of mass. Part of this mass is accreted by the MS compan-

ion through an accretion disk. The disk launches two jets that form the lobes. The process is accompanied by high luminosity that makes the event an ILOT.

3 THE NEGATIVE JET FEEDBACK MECHANISM

Consider a flow structure where a large gas reservoir supplies mass to an accretion disk that launches jets. If these jets are not too narrow, they can interact with the reservoir and expel and heat the mass residing there. This heating and/or ejection of reservoir gas reduces the mass supply rate to the accretion disk, hence lowering the jets' power, and even shutting-off jet formation completely. Jets can affect the ambient gas very efficiently by getting shocked to high temperature and inflating hot bubbles (e.g., Hillel & Soker 2016 and references therein). The bubble has a larger cross section to push and expel ambient gas, also in directions away from the direction of the jet. The inflation of the bubble is accompanied by the formation of many vortices that mix part of the hot gas with the cooler ambient gas (e.g., Hillel & Soker 2016). This results in an efficient heating of the ambient gas. This entire process can convert kinetic energy to thermal energy and then to radiation.

This negative JFM was studied for a variety of astrophysical objects in the literature. These systems are listed in Table 1. The table does not include PNe, because for them the interaction of the jets is on very large scales and it does not trigger a feedback. Only if the shaping takes place close to the binary system, like if the nebula is expelled during grazing envelope evolution (GEE) that might also involve an ILOT (see Soker 2016), does feedback occur. It is listed here under GEE. We compare the size and gravitational potential of the accreting body in each type of object with those of the reservoir of gas, R_a , Φ_a , R_{res} and Φ_{res} , respectively.

Soker et al. (2013) made comparisons of the JFM operating during galaxy formation, in cooling flows in clusters of galaxies, during the common envelope evolution (CEE), in PNe, and in core collapse SNe (CCSNe). Boosted by the results of the Chandra and XMM-Newton X-ray observatories, there have been many papers in the last fifteen years on the operation of a JFM in galaxy formation and cooling flow clusters (McNamara & Nulsen 2012; Soker et al. 2013 and references therein). In recent years there have been suggestions for the operation of a JFM in the explosion of massive stars in CCSNe and during CEE. The jet-feedback mechanism for the explosion of all CCSNe is termed the jittering-jets model (Papish & Soker 2011, 2012, 2014a,b; Gilkis & Soker 2014, 2015a,b; Papish et al. 2016).

Numerical simulations encountered difficulties in expelling the envelope gas during the CEE, as a large fraction of the envelope stays bound to the system even after a substantial spiraling-in of the two stars (e.g., Sandquist et al. 1998; Lombardi et al. 2006; De Marco et al. 2011; Passy et al. 2012; Ricker & Taam 2012, but see Nandez et al. 2015). These difficulties and the problems with the α_{CE} -prescription (e.g., Soker 2013a) lead to the sugges-

Table 1 Comparing Feedback Properties in Astrophysical Objects

Object type	Accreting object	R_a (cm)	Φ_a (km s^{-1}) ²	R_{res} (cm)	Φ_{res} (km s^{-1}) ²	Φ_a/Φ_{res}
Galaxy formation	SMBH	10^{11-14}	c^2	10^{20-23}	$(300)^2$	$\approx 10^6$
Cluster cooling flows	SMBH	10^{13-16}	c^2	10^{21-24}	$(1\,000)^2$	$\approx 10^5$
	NS	10^6	$(100\,000)^2$	10^9	$(10\,000)^2$	≈ 100
CCSN						
GEE ¹	MS star	10^{11}	$(500)^2$	10^{13}	$(30)^2$	≈ 100
CEE ^{1,2}	MS star	10^{11}	$(500)^2$	10^{13}	$(30)^2$	≈ 100
ILOTs ²	MS star	10^{11-12}	$(1\,000)^2$	10^{11-13}	$(30 - 1\,000)^2$	$\approx 3 - 100$

Notes: R_a and Φ_a stand for the typical radius of the accreting object and the gravitational potential on its surface respectively. R_{res} and Φ_{res} stand for the typical radius of the reservoir of gas for accretion and the magnitude of the gravitational potential of the reservoir, which is about the energy per unit mass required to expel gas from the system, respectively. c represents the speed of light.

Abbreviations: BH: black hole; CCSN: core-collapse SN; CEE: common envelope evolution; GEE: grazing envelope evolution; NS: neutron star; SMBH: supermassive BH.

¹ We refer here only to a giant primary star and an MS companion. See text for the case of an NS or a BH companion.

² Although in the other objects jets are a crucial ingredient in the evolution, in the CEE and in ILOTs in some cases jets do not occur, or play a small role. Furthermore, the JFM does not operate in all cases, even if jets do exist.

tion that in many cases envelope ejection is facilitated by jets launched by the more compact companion (Soker 2004; Kashi & Soker 2011; Soker 2013a, 2014). Armitage & Livio (2000) and Chevalier (2012) studied CE ejection by jets launched from a neutron star (NS) companion but not as a general CE ejection process.

An efficient JFM might even prevent the formation of a CEE. Instead, the compact companion spirals-in while grazing the envelope of the giant star, in what is termed the GEE (Soker 2015). If the companion is on an eccentric orbit and grazes the envelope, or even forms a temporary common envelope, it can accrete at a high rate, releasing gravitational energy that is observed as an ILOT. As such, the JFM can operate in ILOTs, as we propose below. We note that Ivanova et al. (2013) mention that the ejection of the envelope through a CCE can lead to an ILOT event, but they do not mention jets.

Launching jets by an MS star in the GEE and the CEE requires that MS stars can accrete at high rates reaching $0.001-0.1 M_{\odot} \text{ yr}^{-1}$ and launch jets. It seems that MS stars can indeed accrete mass at high rates if the jets that are launched by the accretion disk or belt remove most of the accreted energy and angular momentum (Shiber et al. 2015). As well, even if the specific angular momentum of the accreted gas is below the value needed to form a Keplerian accretion disk, but not by much, the accretion belt formed around the MS star might launch jets (Schreier & Soker 2016). An accretion belt is defined here as a sub-Keplerian accretion flow on the surface of the accreting body, with mass concentration closer to the equatorial plane. Schreier & Soker (2016) argue that jets might be blown from the polar regions of the accretion belt.

The effect of the JFM can be quantified by the ratio between the gravitational potential energy of the mass accreted onto the surface of the compact body and that of the ambient gas in the reservoir. If this ratio is large, as in galaxies and clusters of galaxies, then a small amount of accreted mass can launch jets that have a large impact on the ambient gas. We find that for many ILOTs this ratio is smaller than in the other types of objects listed in Table 1. This implies that the JFM in ILOTs is less efficient than in most other cases listed in Table 1. A large fraction of the mass available in the reservoir is accreted in a typical ILOT event.

We note that in the case of ILOTs, jets can interact with gas residing close to the accreting star, hence leading to the operation of the JFM, or with gas residing further out that is not part of the reservoir. The interaction with gas residing further out, but in a still optically thick region, converts kinetic energy to thermal energy, and then radiation. Namely, the interaction can increase the luminosity of the ILOTs.

We turn now to discuss several settings of ILOTs powered by accreting MS stars, and the different manifestations of a JFM in each one of them. The three different scenarios differ mainly in the time period during which the accretion process takes place, and in the reservoir of the accreted mass onto the MS star.

(1) *An ILOT event at a periastron passage.* In this scenario the accretion phase lasts for a fraction of the orbit. The accreted gas originates from one side of the bloated atmosphere of a giant star. For these, the JFM does not destroy the entire mass reservoir, and if the MS companion survives, then the outburst might repeat itself. The best ex-

ample is the GE of η Car, where there were at least two outbursts separated by ~ 5.2 years in the orbital period. Both mass removal and mass accretion act to change both the eccentricity and orbital separation, but in opposite directions. Whether the eccentricity and the orbital separation increase or decrease depends on the details of the interaction, and on the mass loss rate far from periastron, when accretion does not take place or has a small rate (see Kashi & Soker 2010b). In the GE of η Car, according to the HAPI model, the companion accreted mass mainly at periastron passages. The distance between the two stars at periastron passages was $a_p \approx 300R_\odot$. The companion could have entered the extended and tidally distorted envelope of the primary LBV star, and then exited it. This may be termed GEE. Most of the accreted mass came from the equatorial plane. Some mass though, could have been accreted from all directions including from above and below the companion, at a typical distance from the secondary star of $\approx 50\text{--}100 R_\odot$. The radius of the secondary star is $R_a \approx 20 R_\odot$. When the mass of the primary star is included, we find $\Phi_a/\Phi_{\text{res}} \approx 3$. This relatively low value and the small fraction of reservoir gas residing along the polar directions make the JFM less efficient than in most objects listed in Table 1. Still, we hold that the JFM can operate in giant eruptions of very massive stars.

(2) *The JFM in a fall back gas.* In this scenario the JFM takes place for a long time, relative to the dynamical time, after the outburst was triggered. The accreted gas is a fall back gas from the violent event, e.g., a merger process. This JFM is expected to operate once after one violent event. As not much mass falls back, and the JFM here will not change the binary parameters much. The estimated ejected mass in the 1988 outburst of M31 RV was $\approx 0.001\text{--}0.1 M_\odot$ with an expansion velocity of $\approx 100\text{--}500 \text{ km s}^{-1}$ (Mould et al. 1990). Based on some similarities with V838 Mon, Soker & Tyndra (2003) suggested that the M31 RV eruption was caused by a merger-burst event. In Kashi & Soker (2010b) we raised the possibility that a merging process might be replaced with a rapid mass transfer episode in a binary system. We considered a small ejected mass that quickly became optically thin. Part of the ejected material might not have reached the escape velocity, and fell back toward the star, or the binary system if the companion survived the event. The inflated envelope and the gas that did not reach escape velocity fell back toward the star. Instead of a long-lived inflated envelope as in the case of V838 Mon, we argued, an accretion disk was formed after about a year. Because of the high specific angular momentum in the binary system the fall back gas formed an accretion disk around the accreting star. The material closer to the center formed an accretion disk before the outer parts of the envelope had collapsed.

Here we add that such a scenario can lead to the onset of the JFM. The disk from the fall back gas might have launched jets. The jets could have expelled some of the outer parts of the envelope that did not form a disk yet, hence lowering the amount of gas accreted to the center.

This is a negative JFM process. It might act in general cases of merger-bursts where a large envelope is inflated, and in addition the gas that continues to be accreted onto the central star has sufficient specific angular momentum to form an accretion disk that launches two jets. Namely, even if most of the mass in a red transient (a merger-burst) is lost via the outer Lagrange point, e.g., Pejcha et al. (2016), jets might still be formed. This can be after the merger process as outlined above, or before the full merger when the denser star accretes gas from the other star via an accretion disk.

The ratio Φ_a/Φ_{res} depends on the mass distribution in the envelope that is formed after the merger. Even if it is an extended envelope, most of the reservoir mass might reside close to the accreting star, resulting in $\Phi_a/\Phi_{\text{res}} \approx 10$. As well, due to the high angular momentum of a merger event, mass is concentrated toward the equatorial plane, hence it is less affected by the polar jets. Overall, the JFM is not extremely efficient in this setting. Still, it plays some role.

We note that in the merger simulation of Nandez et al. (2014) no accretion disk was formed. We do not claim that jets are formed in all merger-bursts, but in many cases they might form.

(3) *Spiral-out grazing envelope evolution.* In this scenario the accretion phase lasts for the entire orbit, and for many orbits. The accreted gas originates from the outer parts of the giant’s envelope and near its equator. Mass removal can be significant, hence acting to increase orbital separation. But as the JFM requires the MS companion to accrete mass from the envelope, even if orbital separation increases, it will not be by much, as the companion cannot get too far from the envelope. Basically, the companion might end at an orbital separation of about the size of the giant primary star, $\approx 1 \text{ AU}$. The removal of gas by jets can have an indirect influence through dynamical effects. This is known to occur for example during galaxy formation. A rapid removal of baryonic mass by AGN activity reduces the depth of the gravitational well, hence also causing the dark matter to expand (e.g., Martizzi et al. 2013). This further reduces the gravitational well, and hence acts to further lower the density of gas in the center of the galaxy. This in turn acts to reduce the accretion rate to the central SMBH.

Mass loss by either star in a binary system and mass transfer between them changes the orbital parameters. The operation of the JFM in removing gas from a giant envelope (the primary) can have a dynamical effect. The jets remove mass above and below the trajectory of the accreting compact star through the giant envelope, as depicted in Figure 2. As the center of mass is between the two stars, in the case that the secondary star is not much lighter than the primary star, the removed mass is closer to an axis through the center of mass and perpendicular to the equatorial plane (depicted by a dashed line) than most of the rest of the giant’s surface. This implies that the removed envelope mass has a lower value of specific angular momentum than the average of the giant’s surface. Since in a

strong binary interaction it is expected that the mass loss will be concentrated toward the equatorial plane, we find that the JFM removes mass with a lower specific angular momentum than that from an equatorial mass loss from the primary star. Therefore, the mass removal by jets has a less pronounced effect on reducing the orbital separation. In addition, the energy used to expel the envelope mass comes from the mass accretion onto the companion, and not from the orbital energy. These two properties, of a relatively low specific angular momentum of the removed gas and using the accretion energy to remove gas, do not act strongly to reduce the orbital separation. Therefore, the mass loss process in the JFM acts to increase the orbital separation. On the other hand, if the accreting secondary star is much lighter than the primary giant star, mass transfer acts to reduce the orbital separation.

If the accretion rate started at a high rate and later decreased, there may be enough gas in the disk to launch a jet. The mass removal by the jet can supersede the decreasing accretion rate, deplete the reservoir and consequently stop the mass transfer. This would cause an increase of the orbital period. If the binary has an eccentric orbit, eccentricity can increase as well. This spiral-out evolution resulting from the JFM operating in binary stars will be studied in detail in a forthcoming paper.

4 SUMMARY

We explored some aspects of the physics of ILOTs under the assumption that they are powered by a high mass accretion rate on to an MS or a star that is slightly evolved off the MS. In this high-accretion-power ILOTs (HAPI) model one star in a binary system accretes mass from a companion. The companion can survive or be completely destroyed in a merger-burst event.

In Section 2.1 we defined ILOTs as the general group of gap objects, between novae and SNe, that are not Type Ia SNe or related objects. We also classified ILOTs into three subgroups according to the mass transfer process. We updated the ETD where ILOTs occupy a stripe, termed the OTS (Fig. 1). The upper boundary of the OTS can be accounted for by accretion via an accretion disk around an MS star. This upper boundary was derived in Section 2.2 (Eq. (4)). Some implications of the HAPI model were discussed in Section 2.3. In particular, we reiterate an earlier result that the masses of the two stars composing the LBV binary system η Car are much more massive than what is usually assumed based only on the Eddington luminosity limit.

Our most significant new claim is that in some cases ILOTs are regulated to some degree by a negative feedback mechanism mediated by jets. In this JFM the jets expel some mass from the ambient gas reservoir of the accretion disk. This in turn reduces and/or shortens the mass accretion rate. In Table 1 we compared some properties of the JFM of ILOTs with other types of astrophysical objects. In Section 3 we discussed three examples of the possible operation of the JFM in ILOTs.

The examples listed in Section 3 show that the JFM in ILOTs is less efficient than in most of the other types of objects listed in Table 1 for two reasons. (i) The value of the ratio of gravitational potential on the mass accreting body to that in the reservoir, Φ_a/Φ_{res} , is typically lower than in other types of objects. This implies that the jets are required to be more massive to remove a given amount of reservoir gas. (ii) Because the interaction occurs relatively close to the accreting objects, the high value of the specific angular momentum of the accreted gas implies that it tends to flow closer to the equatorial plane. As the jets are launched along the polar directions, they interact with a smaller fraction of the ambient reservoir gas than in a spherical distribution.

As more ILOTs are being discovered we continue to populate the ETD¹ and learn more about them. Further work is required to quantify the outcome of the JFM. Numerical simulations will be the next step. These can show that the jets actually cause the depletion of the mass reservoir. Most relevant is the study of the newly proposed GEE, that requires 3D hydrodynamical numerical simulations.

Acknowledgements We thank an anonymous referee for helpful suggestions. AK acknowledges support provided by the National Science Foundation through grant AST-1109394. AK would like to thank the Technion for their generous hospitality, where part of this work was done.

References

- Adams, S. M., Kochanek, C. S., Prieto, J. L., et al. 2015, arXiv:1511.07393
- Akashi, M., & Soker, N. 2013, MNRAS, 436, 1961
- Arbour, R., & Boles, T. 2008, Central Bureau Electronic Telegrams, 1234
- Armitage, P. J., & Livio, M. 2000, ApJ, 532, 540
- Bear, E., Kashi, A., & Soker, N. 2011, MNRAS, 416, 1965
- Berger, E., Foley, R., & Ivans, I. 2009a, The Astronomer's Telegram, 2184
- Berger, E., Soderberg, A. M., Chevalier, R. A., et al. 2009b, ApJ, 699, 1850
- Bond, H. E., Bedin, L. R., Bonanos, A. Z., et al. 2009, ApJ, 695, L154
- Botticella, M. T., Pastorello, A., Smartt, S. J., et al. 2009, MNRAS, 398, 1041
- Boumis, P., & Meaburn, J. 2013, MNRAS, 430, 3397
- Chevalier, R. A. 2012, ApJ, 752, L2
- Clyne, N., Redman, M. P., Lloyd, M., et al. 2014, A&A, 569, A50
- Damineli, A. 1996, ApJ, 460, L49
- De Marco, O., Passy, J.-C., Moe, M., et al. 2011, MNRAS, 411, 2277

¹ An updated version of the ETD is available at <http://physics.technion.ac.il/ILOT/>

- De Marco, O., et al. 2014, in *Asymmetrical Planetary Nebulae VI Conference*, 1, 122
- De Marco, O. 2015a, *EAS Publications Series*, 71, 357 (<http://poe2015.sciencesconf.org/resource/page/id/16>)
- De Marco, O. 2015b, *Workshop: Stellar End Products: The Low Mass - High Mass Connection*, (<http://www.eso.org/sci/meetings/2015/STEPS2015/program.html>)
- della Valle, M., & Livio, M. 1995, *ApJ*, 452, 704
- Drake, A. J., Howerton, S., McNaught, R., et al. 2012, *The Astronomer's Telegram*, 4334
- Figer, D. F., Najarro, F., Morris, M., et al. 1998, *ApJ*, 506, 384
- Gilkis, A., & Soker, N. 2014, *MNRAS*, 439, 4011
- Gilkis, A., & Soker, N. 2015a, *ApJ*, 806, 28
- Gilkis, A., & Soker, N. 2015b, arXiv:1505.05756
- Hajduk, M., van Hoof, P. A. M., & Zijlstra, A. A. 2013, *MNRAS*, 432, 167
- Hajduk, M., Zijlstra, A. A., van Hoof, P. A. M., et al. 2007, *MNRAS*, 378, 1298
- Hillel, S., & Soker, N. 2016, *MNRAS*, 455, 2139
- Humphreys, R. M., & Martin, J. C. 2012, in *Astrophysics and Space Science Library*, 384, *Eta Carinae and the Supernova Impostors*, eds. K. Davidson, & R. M. Humphreys, 1
- Ivanova, N., Justham, S., Avendano Nandez, J. L., & Lombardi, J. C. 2013, *Science*, 339, 433
- Kamiński, T., Menten, K. M., Tylenda, R., et al. 2015, *Nature*, 520, 322
- Kankare, E., Kotak, R., Pastorello, A., et al. 2015, *A&A*, 581, L4
- Kashi, A. 2010, *MNRAS*, 405, 1924
- Kashi, A., Frankowski, A., & Soker, N. 2010, *ApJ*, 709, L11
- Kashi, A., & Soker, N. 2009, *New Astron.*, 14, 11
- Kashi, A., & Soker, N. 2010a, *ApJ*, 723, 602
- Kashi, A., & Soker, N. 2010b, arXiv:1011.1222
- Kashi, A., & Soker, N. 2011, *MNRAS*, 417, 1466
- Kashi, A., Soker, N., & Moskovitz, N. 2013, *MNRAS*, 436, 2484
- Kasliwal, M. M. 2011, *Bulletin of the Astronomical Society of India*, 39, 375
- Kasliwal, M. M. 2013, in *IAU Symposium*, 281, *Binary Paths to Type Ia Supernovae Explosions*, eds. R. Di Stefano, M. Orio, & M. Moe, 9
- Kasliwal, M. M., Kulkarni, S. R., Arcavi, I., et al. 2011, *ApJ*, 730, 134
- Kochanek, C. S. 2011, *ApJ*, 741, 37
- Kulkarni, S. R., Ofek, E. O., Rau, A., et al. 2007, *Nature*, 447, 458
- Kulkarni, S. R., & Kasliwal, M. M. 2009, in *Astronomy*, 2010, *astro2010: The Astronomy and Astrophysics Decadal Survey*
- Levesque, E. M., Stringfellow, G. S., Ginsburg, A. G., Bally, J., & Keeney, B. A. 2014, *AJ*, 147, 23
- Lombardi, Jr., J. C., Proulx, Z. F., Dooley, K. L., et al. 2006, *ApJ*, 640, 441
- Margutti, R., Milisavljevic, D., Soderberg, A. M., et al. 2014, *ApJ*, 780, 21
- Martin, J. C., Hamsch, F.-J., Margutti, R., et al. 2015, *AJ*, 149, 9
- Martizzi, D., Teyssier, R., & Moore, B. 2013, *MNRAS*, 432, 1947
- Mason, E., Diaz, M., Williams, R. E., Preston, G., & Bensby, T. 2010, *A&A*, 516, A108
- Mauerhan, J. C., Smith, N., Filippenko, A. V., et al. 2013, *MNRAS*, 430, 1801
- Maza, J., Hamuy, M., Antezana, R., et al. 2009, *Central Bureau Electronic Telegrams*, 1928
- Mcley, L., & Soker, N. 2014, *MNRAS*, 440, 582
- McNamara, B. R., & Nulsen, P. E. J. 2012, *New Journal of Physics*, 14, 055023
- Meaburn, J., Lloyd, M., Vaytet, N. M. H., & López, J. A. 2008, *MNRAS*, 385, 269
- Mehner, A., Baade, D., Rivinius, T., et al. 2013, *A&A*, 555, A116
- Monard, L. A. G. 2008, *IAU Circ.*, 8946
- Mould, J., Cohen, J., Graham, J. R., et al. 1990, *ApJ*, 353, L35
- Nandez, J. L. A., Ivanova, N., & Lombardi, Jr., J. C. 2014, *ApJ*, 786, 39
- Nandez, J. L. A., Ivanova, N., & Lombardi, J. C. 2015, *MNRAS*, 450, L39
- Ofek, E. O., Kulkarni, S. R., Rau, A., et al. 2008, *ApJ*, 674, 447
- Ofek, E. O., Sullivan, M., Cenko, S. B., et al. 2013, *Nature*, 494, 65
- Papish, O., & Soker, N. 2011, *MNRAS*, 416, 1697
- Papish, O., & Soker, N. 2012, *MNRAS*, 421, 2763
- Papish, O., & Soker, N. 2014a, *MNRAS*, 438, 1027
- Papish, O., & Soker, N. 2014b, *MNRAS*, 443, 664
- Papish, O., Gilkis, A., & Soker, N. 2016, arXiv:1508.00218
- Passy, J.-C., De Marco, O., Fryer, C. L., et al. 2012, *ApJ*, 744, 52
- Pastorello, A., Botticella, M. T., Trundle, C., et al. 2010, *MNRAS*, 408, 181
- Pastorello, A., Cappellaro, E., Inserra, C., et al. 2013, *ApJ*, 767, 1
- Pejcha, O., Metzger, B. D., & Tomida, K. 2016, *MNRAS*, 455, 4351
- Prieto, J. L., Sellgren, K., Thompson, T. A., & Kochanek, C. S. 2009, *ApJ*, 705, 1425
- Rau, A., Kulkarni, S. R., Ofek, E. O., & Yan, L. 2007, *ApJ*, 659, 1536
- Ricker, P. M., & Taam, R. E. 2012, *ApJ*, 746, 74
- Sandquist, E. L., Taam, R. E., Chen, X., Bodenheimer, P., & Burkert, A. 1998, *ApJ*, 500, 909
- Schreier, R., & Soker, N. 2016, *RAA (Research in Astronomy and Astrophysics)*, 16, 70
- Shara, M. M., Moffat, A. F. J., & Webbink, R. F. 1985, *ApJ*, 294, 271
- Shara, M. M., Yaron, O., Prialnik, D., Kovetz, A., & Zurek, D. 2010, *ApJ*, 725, 831
- Shiber, S., Schreier, R., & Soker, N. 2015, arXiv:1504.04144
- Smith, N., Ganeshalingam, M., Chornock, R., et al. 2009, *ApJ*, 697, L49

- Smith, N., Mauerhan, J. C., & Prieto, J. L. 2014, *MNRAS*, 438, 1191
- Soker, N., & Tylenda, R. 2003, *ApJ*, 582, L105
- Soker, N. 2004, *New Astron.*, 9, 399
- Soker, N., & Tylenda, R. 2006, *MNRAS*, 373, 733
- Soker, N., & Kashi, A. 2011, arXiv:1107.3454
- Soker, N., & Kashi, A. 2012, *ApJ*, 746, 100
- Soker, N., & Kashi, A. 2013, *ApJ*, 764, L6
- Soker, N., Akashi, M., Gilkis, A., et al. 2013, *Astronomische Nachrichten*, 334, 402
- Soker, N. 2013a, *New Astron.*, 18, 18
- Soker, N. 2013b, arXiv:1302.5037
- Soker, N. 2014, arXiv:1404.5234
- Soker, N. 2015, *ApJ*, 800, 114
- Soker, N. 2016, *New Astron.*, 47, 16
- Szyszkla, C., Zijlstra, A. A., & Walsh, J. R. 2011, *MNRAS*, 416, 715
- Tartaglia, L., Pastorello, A., Taubenberger, S., et al. 2015, *MNRAS*, 447, 117
- Thompson, T. A., Prieto, J. L., Stanek, K. Z., et al. 2009, *ApJ*, 705, 1364
- Tylenda, R., Soker, N., & Szczerba, R. 2005, *A&A*, 441, 1099
- Tylenda, R., & Soker, N. 2006, *A&A*, 451, 223
- Tylenda, R., Kamiński, T., Udalski, A., et al. 2013, *A&A*, 555, A16
- Williams, S. C., Darnley, M. J., Bode, M. F., & Steele, I. A. 2015, *ApJ*, 805, L18
- Yaron, O., Prialnik, D., Shara, M. M., & Kovetz, A. 2005, *ApJ*, 623, 398
- Zijlstra, A. A. 2015, *RMxAA*, 51, 221